iScience

CellPress
OPEN ACCESS

Article

Exploring the role of SWI/SNF complex subunit BAF60c in lipid metabolism and inflammation in fish

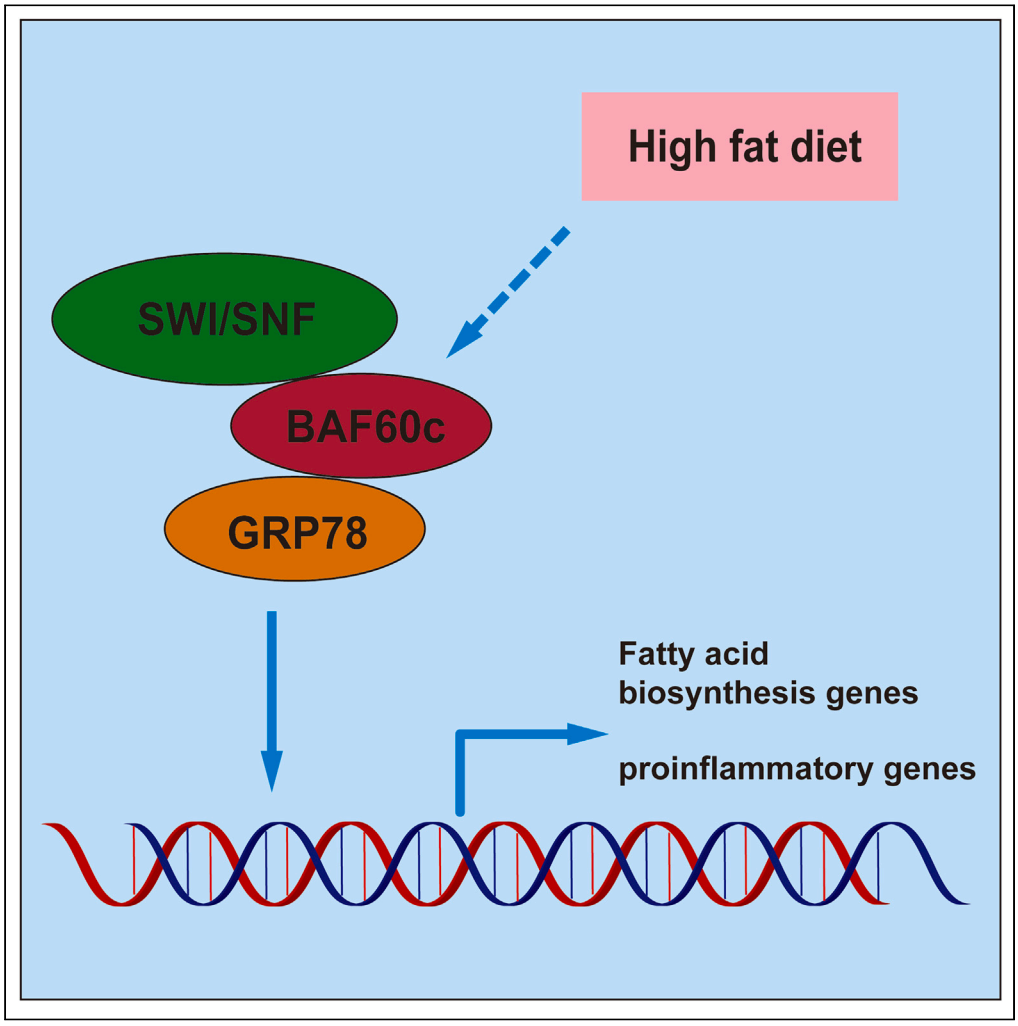

Jie Sun, Qiuxin Yan, Zhihao Zhang, ..., Weijia Li, Kangsen Mai, Qinghui Ai

qhai@ouc.edu.cn

Highlights

First demonstrated that BAF60c can interact with GRP78

Explored the function of BAF60c in lipid metabolism and inflammation in fish

Enriched the BAF60c-interacting protein network

Sun et al., iScience *26*, 108207
November 17, 2023
https://doi.org/10.1016/j.isci.2023.108207

iScience

CellPress
OPEN ACCESS

Article

Exploring the role of SWI/SNF complex subunit BAF60c in lipid metabolism and inflammation in fish

Jie Sun,[1] Qiuxin Yan,[1] Zhihao Zhang,[1] Ting Xu,[1] Ye Gong,[1] Weijia Li,[1] Kangsen Mai,[1,2] and Qinghui Ai[1,2,3,*]

SUMMARY

Chromatin remodeling plays an important role in regulating gene transcription, in which chromatin remodeling complex is a crucial aspect. Brg1/Brm-associated factor 60c (BAF60c) subunit forms a bridge between chromatin remodeling complexes and transcription factors in mammals; hence, it has received extensive attention. However, the roles of BAF60c in fish remain largely unexplored. In this study, we identified BAF60c-interacting proteins by using HIS-pull-down and LC-MS/MS analysis in fish. Subsequently, the RNA-seq analysis was performed to identify the overall effects of BAF60c. Then, the function of BAF60c was verified through BAF60c knockdown and overexpression experiments. We demonstrated for the first time that BAF60c interacts with glucose-regulated protein 78 (GRP78) and regulates lipid metabolism, endoplasmic reticulum (ER) stress, and inflammation. Knockdown of BAF60c reduces fatty acid biosynthesis, ER stress, and inflammation. In conclusion, the results enriched BAF60c-interacting protein network and explored the function of BAF60c in lipid metabolism and inflammation in fish.

INTRODUCTION

Chromatin remodeling plays a vital role in gene transcription, in which the chromatin remodeling complex is an important aspect. SWI/SNF is the first characterized ATP-dependent remodeling complex and is evolutionarily conservative from yeast to mammals.[1,2] The SWI/SNF complex in mammals is also known as the Brg1/Brm-associated factor (BAF) complex. Previous studies demonstrated that the BAF complex was essential for transcriptional regulation, genomic stability, DNA repair, and development and differentiation.[3,4] Furthermore, it has been indicated that the BAF complex can participate in various biological processes, including embryogenesis, cell cycle, and tumorigenesis.[5,6] The BAF complex is composed of a core ATPase subunit (Brg1 or Brm), other modulatory BAF subunits, including BAF155, BAF170, and BAF250, and other auxiliary subunits, such as BAF57 and BAF60.[2,7]

BAF60 has been verified to interact with transcription factors (TFs) and function as a bridge between TFs and other BAF subunits.[8–12] BAF60 contains three isoforms, including BAF60a, BAF60b, and BAF60c, which is encoded by *smarcd1*, *smarcd2*, and *smarcd3*, respectively.[13] Different BAF60 isoforms play specific roles by interacting with different regulators. Previous studies have demonstrated that BAF60a could regulate lipid homeostasis,[11] energy metabolism,[14] and tumor suppression.[15] Additionally, BAF60c has been identified to regulate heart development,[12,16,17] muscle development,[18–20] and glycolytic metabolism.[21,22] Despite the crucial role of BAF60c, its investigation in fish remains largely unexplored.

Glucose-regulated protein 78 (GRP78), also known as heat shock protein family A member 5 or the immunoglobulin heavy-chain-binding protein (BiP), belongs to the heat shock protein 70 family and refers to as an endoplasmic reticulum (ER) molecular chaperone. GRP78 was an important regulator of ER homeostasis.[23] Prior studies have demonstrated that GRP78 played multiple roles, such as regulating apoptosis[24–27] and autophagy,[28–30] participating in cancer and tumor metabolism,[31–33] mediating energy metabolism,[34–37] regulating inflammatory response,[38–40] and so on. However, the interaction between BAF60c and GRP78 has not been reported. The function of them also needs further research.

Despite being lower vertebrates to mammals, fish possess evolutionarily conserved systems for nutrient-sensing and immune response pathways.[41] High-fat diet (HFD) is extensively used in fish farming because of the protein-sparing effect,[42] while lipid overload can cause metabolic disorders and fat accumulation in liver[43] and induce inflammation.[44] However, the regulatory role of BAF60c in lipid metabolism and inflammation needs to be further investigated, and the role of GRP78 also remains unexplored. Large yellow croaker (*Larimichthys crocea*) is a vital mariculture species in China and can be used as a terrific experimental model animal. Therefore, this study was designed to identify

[1]Key Laboratory of Aquaculture Nutrition and Feed (Ministry of Agriculture and Rural Affairs) & Key Laboratory of Mariculture (Ministry of Education), Ocean University of China, 5 Yushan Road, Qingdao, Shandong 266003, People's Republic of China
[2]Laboratory for Marine Fisheries Science and Food Production Processes, Qingdao National Laboratory for Marine Science and Technology, 1 Wenhai Road, Qingdao, Shandong 266237, People's Republic of China
[3]Lead contact
*Correspondence: qhai@ouc.edu.cn
https://doi.org/10.1016/j.isci.2023.108207

the global interaction proteins of BAF60c in fish. Moreover, the present study also aimed to elucidate the biological functions of BAF60c. This study might develop an in-depth understanding of the interacting protein network of BAF60c and further determine the important functions of BAF60c in lipid metabolism and inflammation in fish. Moreover, this study may provide theoretical basis for alleviating the abnormal lipid deposition and inflammation induced by HFD.

RESULTS

Identification of GRP78 as a BAF60c-interacting protein

To determine the function that BAF60c plays in fish, we first cloned *baf60c* (Figure S1A). Then the basic bioinformatic analysis showed that BAF60c was highly conserved (Figures S1B–S1D) (Figure S2). Subcellular localization results indicated that BAF60c was ubiquitously expressed in cell (Figure S1E).

Furthermore, to identify additional BAF60c-interacting factors, we performed HIS pull-down analysis followed by liquid chromatography-tandem mass spectrometry. Kyoto Encyclopedia of Genes and Genomes (KEGG) enrichment analysis indicated that the identified proteins were enriched in metabolic pathways, protein processing in endoplasmic reticulum, biosynthesis of secondary metabolites, and so on (Figure 1A). Gene Ontology (GO) enrichment analysis found that the identified proteins were mainly involved in cellular process, metabolic process, and binding (Figure 1B). Furthermore, results showed that 407 specific proteins were identified (Figure 1C). Among all identified proteins, GPR78 was chosen for further experiment for its important functions in ER. We detected an interaction between GRP78 and BAF60c in cells by coimmunoprecipitation (Figure 2A). Moreover, BAF60c-GFP distinctly appeared to colocalize with GRP78-RFP, as shown by confocal microscopy (Figure 2B).

BAF60c regulated GRP78 expression

In order to figure out the relationship between BAF60c and GRP78, we conducted knockdown or overexpression experiments. BAF60c-siRNA in macrophages significantly decreased the expression of *baf60c*. Meanwhile, the expression of *grp78* was also downregulated significantly ($p < 0.05$) (Figure 3A). The result in hepatocytes was the same as those in macrophages. BAF60c-siRNA significantly decreased the expression of *baf60c* and *grp78* ($p < 0.05$) (Figure 3B). Additionally, overexpression of BAF60c in hepatocytes significantly increased the expression of *baf60c* and *grp78* ($p < 0.05$) (Figure 3C). GRP78 agonist (BiP) treatment in macrophages significantly upregulated the expression of *grp78* ($p < 0.05$), but the expression of *baf60c* was not remarkably increased (Figure 3D). Moreover, the protein levels of BAF60c were not changed after BiP treatment (Figure 3E). Furthermore, GRP78 inhibitor (HM03) treatment in macrophages significantly decreased the expression of *grp78* ($p < 0.05$) (Figure 3F). However, the mRNA and protein levels of BAF60c were not remarkably changed after the HM03 treatment (Figures 3F and 3G).

Further function analysis of BAF60c through RNA sequencing

BAF60c can regulate the expression of GRP78, suggesting the potential function of BAF60c in ER. Then, to identify the overall effects of BAF60c, we carried out RNA sequencing analysis. After BAF60c-siRNA treatment, a total of 2204 upregulated genes and 2221 downregulated genes were identified compared to the control group (Figures 4A and 4B). GO enrichment analysis found that the differential genes were mainly involved in protein transport, establishment of protein localization, peptide transport, and organic acid metabolic process (Figure 4C). KEGG enrichment analysis showed that the differential genes were enriched in proteasome, cell cycle, various diseases and cancers, and protein processing in endoplasmic reticulum (Figure 4D). In addition, genes in fatty acid biosynthesis pathway were downregulated (Figure S3). However, genes in fatty acid degradation pathway were upregulated (Figure S4).

Knockdown of BAF60c reduced fatty acid biosynthesis, ER stress, and inflammation *in vitro*

In order to verify the previously described results, we carried out the knockdown and overexpression experiments. BAF60c-siRNA in macrophages significantly decreased *xbp1*, *xbp1s*, *chop*, and *atf4* expressions ($p < 0.05$) (Figure 5A). Additionally, the proinflammatory genes, including *il-8*, *il-6*, *il-1β*, *cox2*, and *tnfα*, were significantly downregulated ($p < 0.05$) (Figure 5B). BAF60c-siRNA in hepatocytes significantly downregulated the mRNA levels of *xbp1*, *xbp1s*, *chop*, and *atf4* ($p < 0.05$) (Figure 5C). Furthermore, the mRNA levels of proinflammatory genes were significantly decreased, including *il-6*, *il-1β*, *cox2*, *tnfα*, and *infγ* ($p < 0.05$) (Figure 5D). Moreover, the lipid metabolism-related genes, including *scd*, *srebp*, *apob*, and *lpl*, were significantly decreased, while *cpt1* and *atgl* were significantly increased ($p < 0.05$) (Figure 5E). The protein level of GRP78 was significantly downregulated in BAF60c-siRNA group compared to the control group. Meanwhile, the phosphorylation level of JNK was significantly upregulated ($p < 0.05$) (Figure 5F).

Overexpression of BAF60c in hepatocytes significantly increased the expression of *xbp1*, *xbp1s*, *chop*, *atf6*, and *atf4* ($p < 0.05$) (Figure 6A). Furthermore, the protein level of GRP78 was significantly upregulated in the overexpression group compared to the control group. Meanwhile, the phosphorylation level of ERK was significantly upregulated ($p < 0.05$) (Figure 6B).

Knockdown of BAF60c reduced lipogenesis, ER stress, and inflammation *in vivo*

We next examined the biological function of BAF60c *in vivo* by dsRNA-mediated gene knockdown analysis. The results revealed that intraperitoneal injection of dsRNA for 36 h significantly decreased the expression of *baf60c*, *fas*, *acc*, *scd*, *srebp1*, *pparγ*, *cebpα*, *pparα*, *mtp*, *il-1β*, and *il-8* in the fish liver ($p < 0.05$) (Figure 7A). Hepatic triglyceride levels were also significantly decreased in the liver of

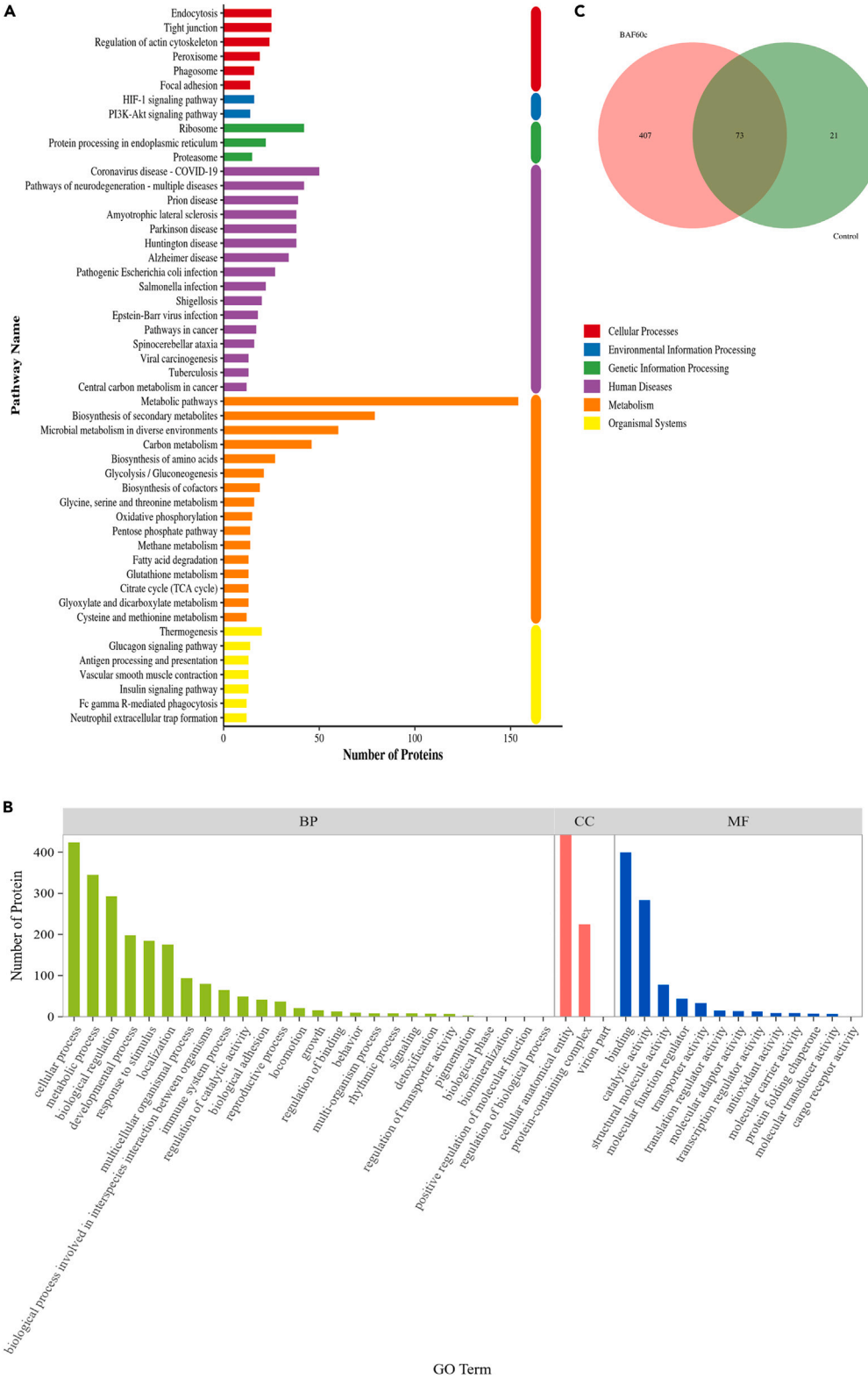

Figure 1. Identification of BAF60c-interacting proteins

(A) KEGG enrichment analysis.

(B) GO enrichment analysis.

(C) Venn diagram. BP: biological process; CC: cellular component; MF: molecular function. See also Figures S1 and S2.

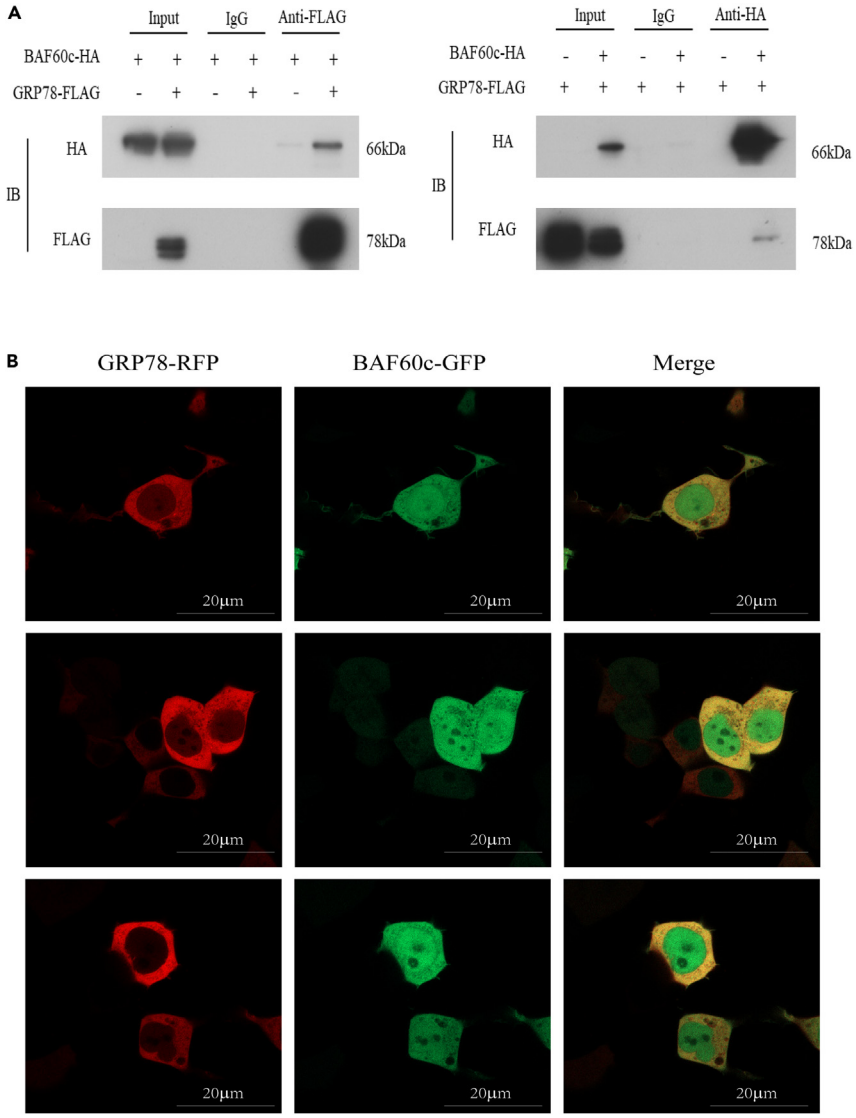

Figure 2. BAF60c interacts with GRP78

(A) Co-IP of HEK293T cells overexpressing BAF60c-HA and GRP78-FLAG.

(B) HEK293T cells were co-transfected with BAF60c-GFP and GRP78-RFP plasmids for 24 h and followed by laser scanning confocal microscopy to observe the colocalization of BAF60c and GRP78. Scale bars, 20 μm.

BAF60c-knockdown fish ($p < 0.05$) (Figure 7B). Additionally, the results showed that injection of dsRNA can alleviate HFD-induced gene expression of *baf60c*, *grp78*, *xbp1*, *atf6*, and *atf4* in the fish head kidney ($p < 0.05$) (Figure 7C). Furthermore, the proinflammatory genes, including *il-8*, *il-1β*, and *cox2*, were also significantly decreased in the dsRNA group compared with the HFD group in the fish head kidney ($p < 0.05$) (Figure 7D). Transmission electron microscopy observation demonstrated that HFD could induce the accumulation of lipid droplets in the fish liver and destroy the structure of the endoplasmic reticulum. However, the injection of dsRNA could alleviate the previously described phenomenon (Figure 7E).

Knockdown of GRP78 reduced fatty acid biosynthesis, ER stress, and inflammation

GRP78-siRNA in macrophages significantly decreased *grp78*, *xbp1*, *xbp1s*, *chop*, *atf4*, and *atf6* expressions ($p < 0.05$) (Figures 8A and 8B). Moreover, the proinflammatory genes, including *il-8*, *il-6*, *il-1β*, *cox2*, and *tnfα*, were significantly downregulated ($p < 0.05$) (Figure 8C). GRP78-siRNA in hepatocytes significantly downregulated the mRNA levels of *grp78*, *xbp1*, *xbp1s*, *chop*, *atf6*, and *atf4* ($p < 0.05$) (Figures 8D and 8E). Furthermore, the mRNA levels of proinflammatory genes were significantly decreased, including *il-8*, *il-1β*, *cox2*, and *infγ* ($p < 0.05$) (Figure 8F). Additionally, the lipid metabolism-related genes, including *fas*, *scd*, *srebp*, *apob*, and *lpl*, were significantly

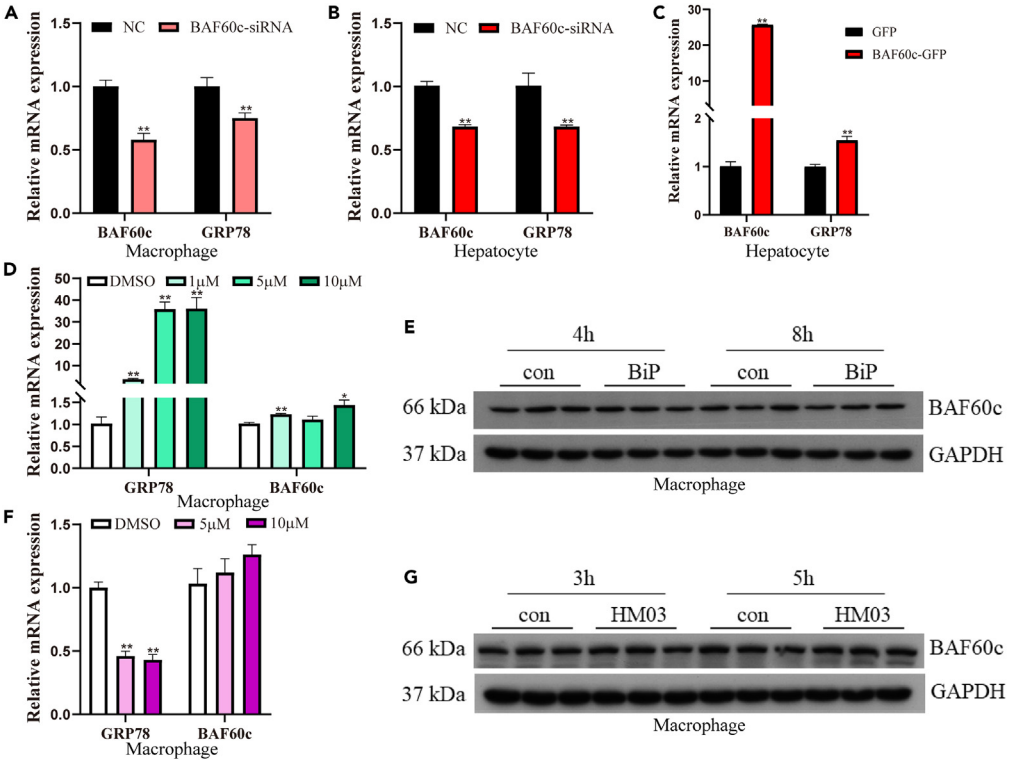

Figure 3. BAF60c regulates GRP78 expression in fish

(A) Relative mRNA expression of BAF60c and GRP78 after BAF60c-siRNA treatment for 36 h in macrophage.

(B) Relative mRNA expression of BAF60c and GRP78 after BAF60c-siRNA treatment for 36 h in hepatocyte.

(C) Relative mRNA expression of BAF60c and GRP78 after overexpression of BAF60c for 24 h in hepatocyte.

(D) Relative mRNA expression of BAF60c and GRP78 after BiP treatment for 4 h with different concentrations in macrophages.

(E) Protein level of BAF60c after 10 μM BiP treatment for 4 and 8 h in macrophages.

(F) Relative mRNA expression of BAF60c and GRP78 after HM03 treatment for 4 h with different concentrations in macrophages.

(G) Protein level of BAF60c after 10 μM HM03 treatment for 3 and 5 h in macrophages. Data are represented as mean ± SEM (n = 3) and were analyzed using independent t test. The "*" means a significant difference ($p < 0.05$), and "**" means a highly significant difference ($p < 0.01$).

decreased, while *cpt1* was significantly increased ($p < 0.05$) (Figure 8G). In conclusion, GRP78-siRNA treatment also reduced fatty acid biosynthesis, ER stress, and inflammation, as the BAF60c-siRNA treatment.

DISCUSSION

SWI/SNF complexes-mediated chromatin remodeling is indispensable for regulating gene transcription. BAF60 subunit of SWI/SNF complexes has been proposed to form a bridge between TFs and chromatin remodeling complexes to regulate gene transcription. BAF60 contains three isoforms and is able to form distinct complexes to regulate diverse cellular functions.[13] In this study, we cloned *baf60c*, and further basic bioinformatic analysis revealed that the BAF60c was highly conservative, suggesting that its function may also be conserved.

Previous researches indicated that BAF60c could interact with various regulators and recruit chromatin remodeling complex to play diverse functions. A previous study showed that BAF60c interacted with heart-related TFs, Gata4 and Tbx5, then recruited SWI/SNF subunits to promote cardiomyocyte differentiation.[45] BAF60c can bind to MyoD, a TF that regulates myogenesis, and further recruits SWI/SNF complexes to remodel chromatin and activate the transcription of MyoD target genes.[18,46] Moreover, BAF60c and Six4 form a transcriptional complex to activate Deptor, then mediated activation of AKT and glycolytic metabolism in a cell-autonomous manner.[21] Furthermore, in response to insulin, BAF60c was phosphorylated and translocated to the nucleus, then interacted with USF-1 and recruited the BAF complex to remodel chromatin and activate lipogenic genes.[47] The present study demonstrated for the first time that BAF60c could interact with GRP78 to play further functions. Moreover, BAF60c could regulate the mRNA and protein level of GRP78 through distinct ways. We speculate that BAF60c may indirectly regulate the mRNA levels of GRP78 by interacting with TF and recruiting chromatin remodeling complex, which was consistent with previous studies.[21,47] Furthermore, consistent with previous studies, BAF60c may also regulate the protein levels of GRP78 through ubiquitination or proteasomal degradation.[48,49] However, whether the interaction between BAF60c and GRP78 affects the degradation of GRP78 needs further exploration.

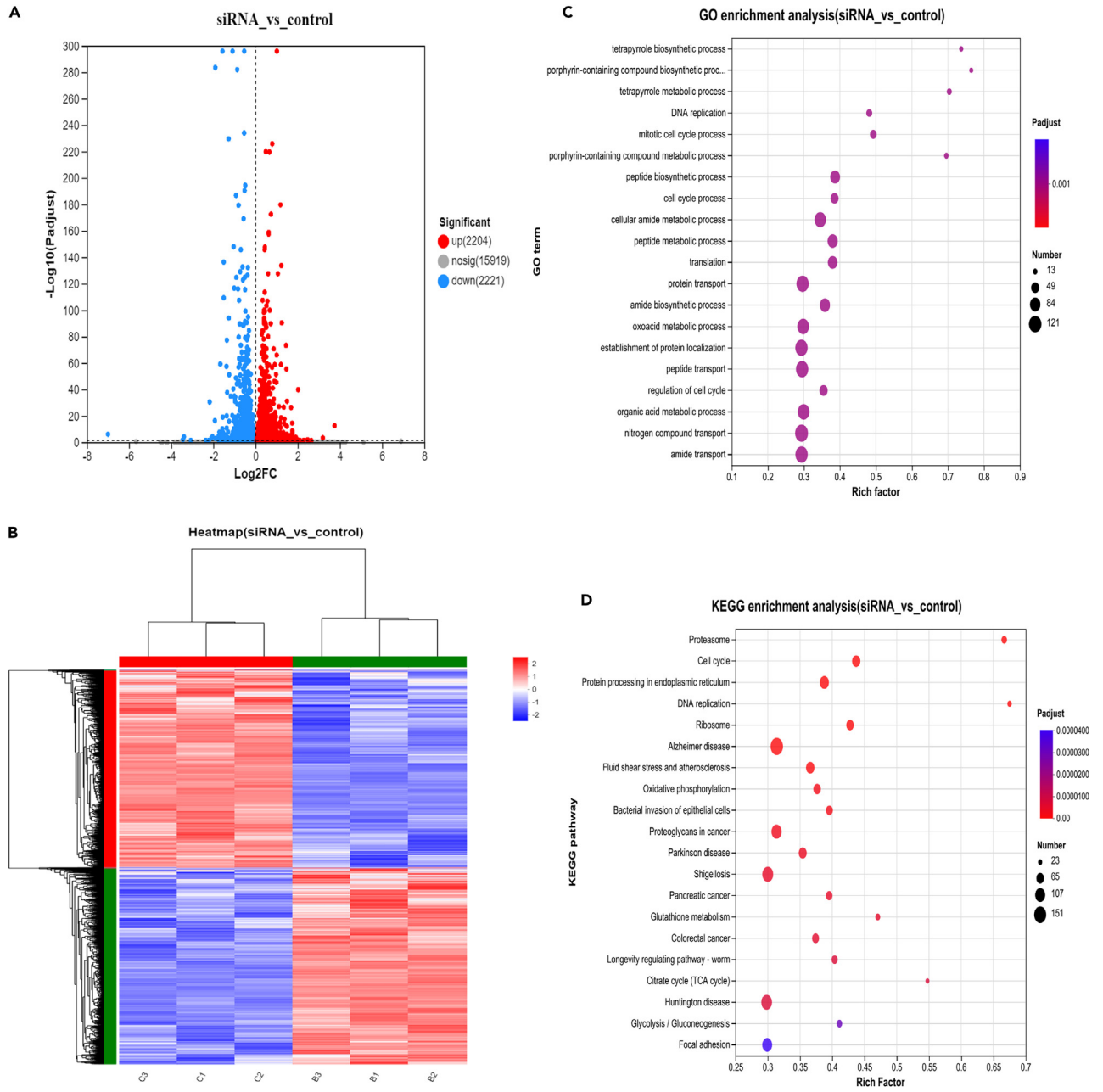

Figure 4. Analysis of differentially expressed genes in transcriptome

(A and B) The differential expressed genes of BAF60c-siRNA vs. control were shown as volcano plot (A) and heatmap (B).

(C) GO enrichment analysis of differentially expressed genes obtained by transcriptomic sequencing analysis of hepatocytes treated with BAF60c-siRNA (n = 3).

(D) KEGG enrichment analysis of differentially expressed genes obtained by transcriptomic sequencing analysis of hepatocytes treated with BAF60c-siRNA (n = 3). See also Figures S3 and S4.

The present study indicated that the BAF60c can regulate lipid metabolism. However, there have been only a few reports on the regulatory roles of BAF60c in lipid metabolism. In response to insulin, BAF60c interacted with USF-1 and activated lipogenic genes.[47] Knockdown of BAF60c could drive global losses in SWI/SNF binding and histone acetylation at active enhancers co-bound by FOXA1, downregulating a network of genes implicated in lipid homeostasis. Meanwhile, loss of BAF60c blunts fatty acid metabolism *in vivo*, positioning BAF60c as an epigenetic regulator of fatty acid metabolism.[50] Previous studies also have indicated that the BAF60a subunit can regulate lipid metabolism. Hepatic inactivation of BAF60a can reduce cholesterol absorption and bile acid synthesis and reduce diet-induced atherosclerosis and hypercholesterolemia.[51] Additionally, PGC-1α mediated the recruitment of BAF60a to PPARα-binding sites and further activated the transcription of

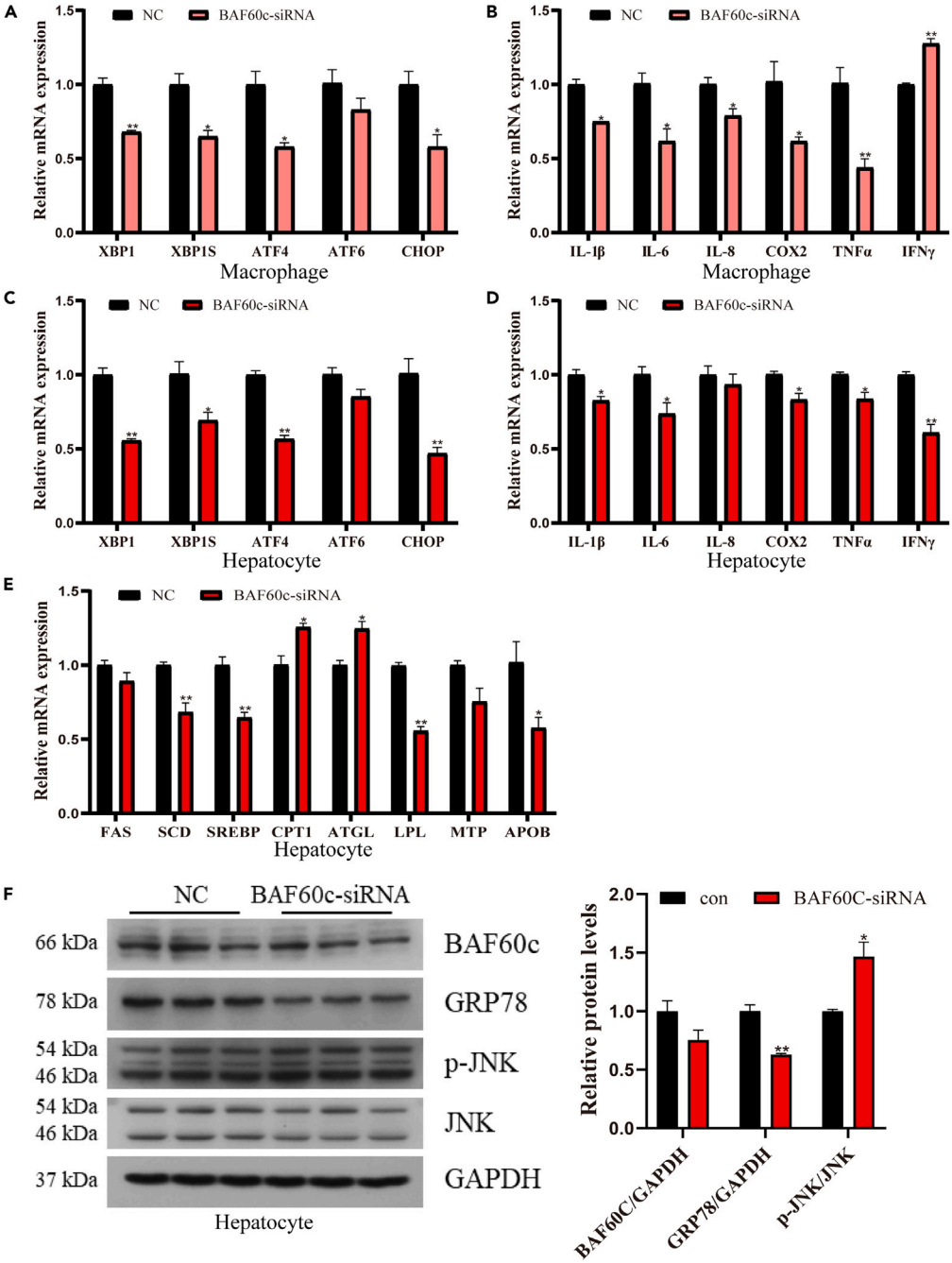

Figure 5. Knockdown of BAF60c in macrophages and hepatocytes can reduce ER stress, inflammation, and fatty acid biosynthesis

(A) Relative mRNA expression of ER stress-related genes after BAF60c-siRNA treatment for 36 h in macrophages.

(B) Relative mRNA expression of inflammatory genes after BAF60c-siRNA treatment for 36 h in macrophages.

(C) Relative mRNA expression of ER stress-related genes after BAF60c-siRNA treatment for 36 h in hepatocytes.

(D) Relative mRNA expression of inflammatory genes after BAF60c-siRNA treatment for 36 h in hepatocytes.

(E) Relative mRNA expression of lipid metabolism-related genes after BAF60c-siRNA treatment for 36 h in hepatocytes.

(F) Protein levels after BAF60c-siRNA treatment for 36 h in hepatocytes. Data are represented as mean ± SEM (n = 3) and were analyzed using independent t test. The "*" means a significant difference ($p < 0.05$), and "**" means a highly significant difference ($p < 0.01$).

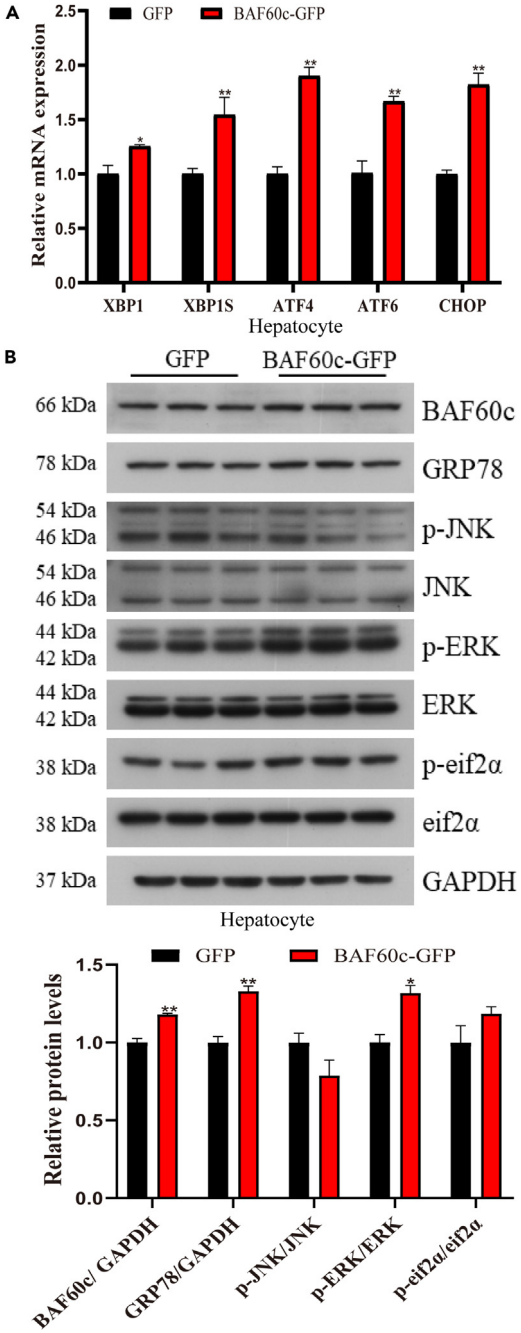

Figure 6. Overexpression of BAF60c in hepatocytes can induce ER stress and inflammation

(A) Relative mRNA expression of ER stress related genes after BAF60c-overexpressing treatment for 24 h in hepatocytes.

(B) Protein levels after BAF60c-overexpressing treatment for 24 h in hepatocytes. Data are represented as mean ± SEM (n = 3) and were analyzed using independent t test. The "*" means a significant difference ($p < 0.05$), and "**" means a highly significant difference ($p < 0.01$).

mitochondrial and peroxisomal fat-oxidation genes to regulate lipid homeostasis.[11] In this study, we revealed that BAF60c interacted with GRP78 and further regulated lipid metabolism. Knockdown of BAF60c can reduce fatty acid biosynthesis and induce fatty acid degradation.

In the present study, we also indicated that BAF60c can regulate ER stress and inflammatory response. These results might be due to BAF60c could regulate the expression of a common ER molecular chaperon, GRP78. Previous studies have shown that GRP78 can regulate ER stress and inflammation. Overexpression of GRP78 can alleviate ER stress.[34,52] Meanwhile, GRP78-siRNA increased ER stress-related genes.[28,53] Furthermore, GRP78 also has been indicated to regulate inflammation.[39,40] To be more specific, adoptive GRP78-DC transfer

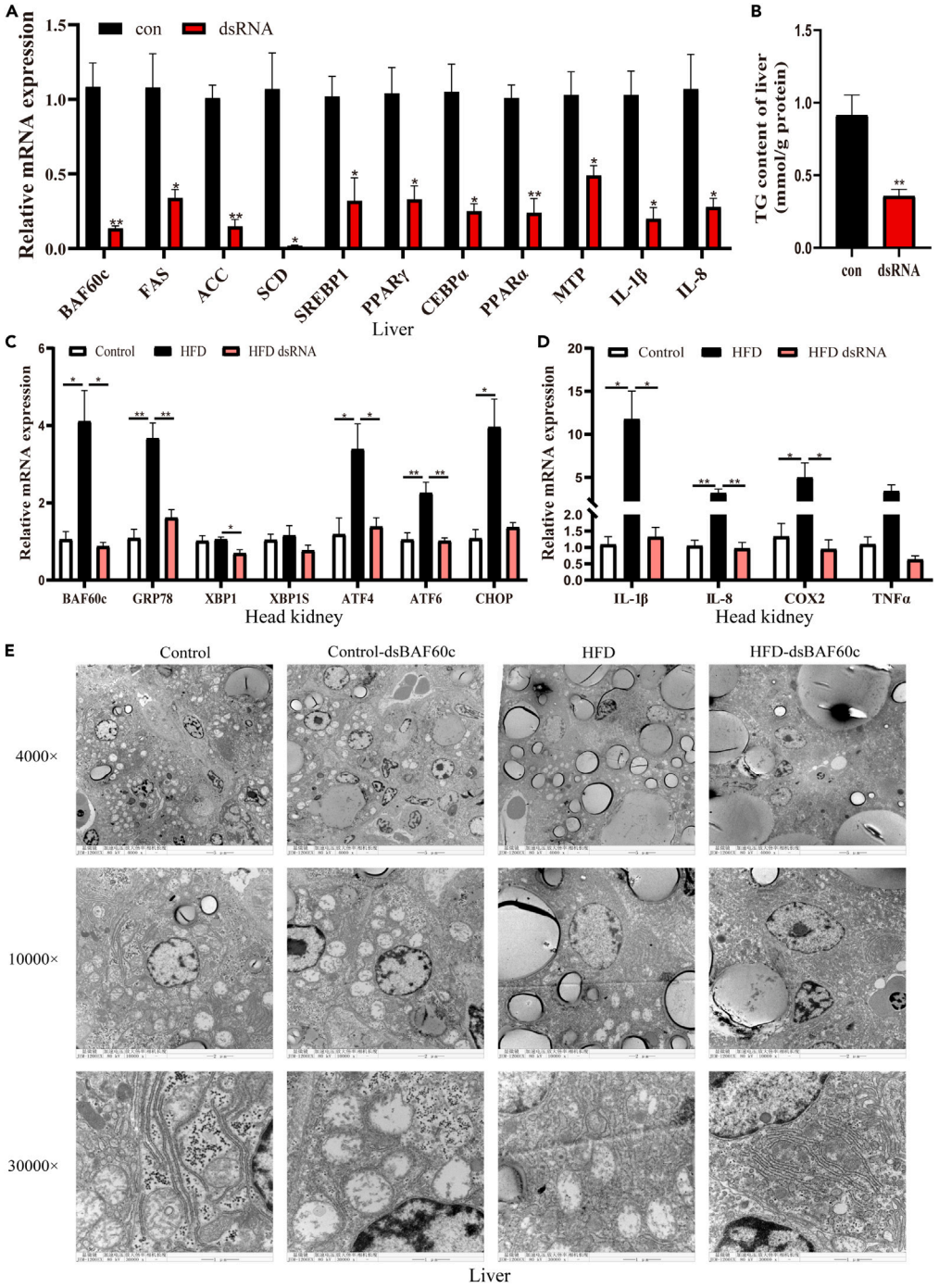

Figure 7. Knockdown of BAF60c can reduce lipogenesis, ER stress, and inflammation *in vivo*

(A) Relative mRNA expression of lipid metabolism-related genes and inflammatory genes in fish liver after injecting BAF60c-dsRNA for 36 h. (B) Hepatic triglyceride (TG) levels after injecting BAF60c-dsRNA for 36 h.

(C) Relative mRNA expression of ER stress-related genes in fish head kidney after injecting BAF60c-dsRNA for 36 h.

(D) Relative mRNA expression of inflammatory genes in fish head kidney after injecting BAF60c-dsRNA for 36 h.

(E) Hepatic transmission electron microscopy (TEM) observation after injecting BAF60c-dsRNA for 36 h. Scale bars, 4000×: 5 μm; 10000×: 2 μm; 30000×: 1 μm. Data are represented as mean ± SEM (n = 3) and were analyzed using independent t test. The "*" means a significant difference ($p < 0.05$), and "**" means a highly significant difference ($p < 0.01$).

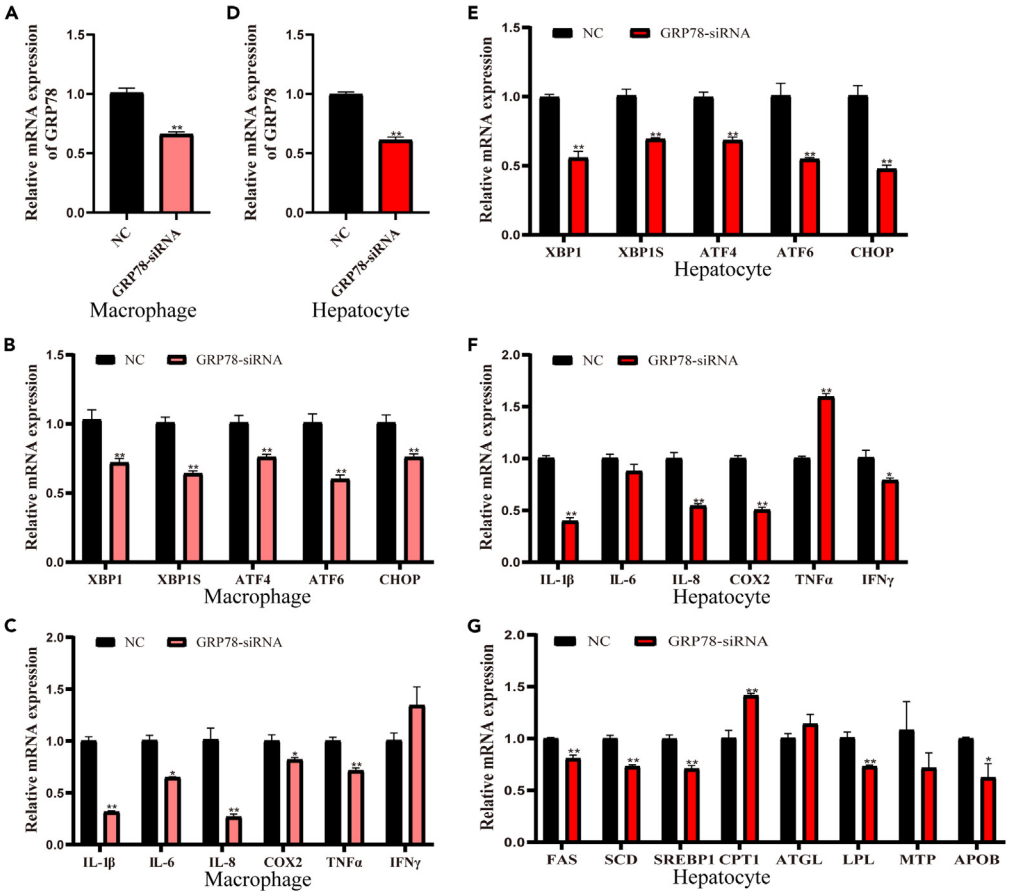

Figure 8. Knockdown of GRP78 in macrophages and hepatocytes can reduce ER stress, inflammation, and fatty acid biosynthesis

(A) Relative mRNA expression of *grp78* after GRP78-siRNA treatment for 36 h in macrophages.

(B) Relative mRNA expression of ER stress-related genes after GRP78-siRNA treatment for 36 h in macrophages.

(C) Relative mRNA expression of inflammatory genes after GRP78-siRNA treatment for 36 h in macrophages.

(D) Relative mRNA expression of *grp78* after GRP78-siRNA treatment for 36 h in hepatocytes.

(E) Relative mRNA expression of ER stress-related genes after GRP78-siRNA treatment for 36 h in hepatocytes.

(F) Relative mRNA expression of inflammatory genes after GRP78-siRNA treatment for 36 h in hepatocytes.

(G) Relative mRNA expression of lipid metabolism-related genes after GRP78-siRNA treatment for 36 h in hepatocytes. Data are represented as mean ± SEM (n = 3) and were analyzed using independent t test. The "*" means a significant difference ($p < 0.05$), and "**" means a highly significant difference ($p < 0.01$).

can resolve inflammation in NOD mice.[40] Moreover, GRP78 can mediate endocytosis of TLR4 by targeting CD14 and alleviate inflammation.[39] However, in the present study, knockdown of BAF60c and GRP78 decreased ER stress-related genes and proinflammatory genes, which might be due to the functional particularity of fish.

In conclusion, we identified the BAF60c-interacting proteins in fish. Further analysis demonstrated for the first time that BAF60c can interact with GRP78 and regulate lipid metabolism, ER stress, and inflammation, which may provide theoretical insights for alleviating the abnormal lipid deposition and inflammation induced by HFD. These results explored the function of BAF60c in fish and demonstrated that BAF60c could regulate ER stress and inflammation for the first time. Additionally, the results enriched the BAF60c-interacting protein network.

Limitations of the study

This study demonstrated for the first time that BAF60c can interact with GRP78 and regulate lipid metabolism, ER stress, and inflammation. The molecular mechanisms need to be further explored, and whether GRP78 mediated the function of BAF60c also needs further investigation.

STAR★METHODS

Detailed methods are provided in the online version of this paper and include the following:

- KEY RESOURCES TABLE
- RESOURCE AVAILABILITY

SUPPLEMENTAL INFORMATION

Supplemental information can be found online at https://doi.org/10.1016/j.isci.2023.108207.

ACKNOWLEDGMENTS

We appreciate Weiwei Dai, Qiuchi Chen, and Yongnan Li for their constructive suggestions for the design of this experiment. We appreciate Fan Chen and Baolin Li for their experimental assistance. We thank Miao Weng and Xiuneng Wang for rearing experimental fish. We also thank Dan Xu, Qiuchi Chen, and Jiamin Li for providing antibodies.

This work was supported by the Scientific and Technological Innovation of Blue Granary (grant number 2018YFD0900402), the Key Program of National Natural Science Foundation of China (grant number 31830103), and the National Natural Science Foundation of China (Shan Dong) (grant number U2106232).

AUTHOR CONTRIBUTIONS

Conceptualization, J.S., K.S.M., and Q.H.A.; formal analysis, J.S.; data curation, J.S., Q.X.Y., Z.H.Z., T.X., and W.J.L.; writing – original draft, J.S.; Writing – review and editing, J.S., Q.X.Y., Z.H.Z., T.X., Y.G., W.J.L., and Q.H.A.; supervision, Q.H.A.; funding acquisition, Q.H.A.

DECLARATION OF INTERESTS

The authors declare no competing interests.

INCLUSION AND DIVERSITY

We worked to ensure diversity in experimental samples through the selection of the cell lines.

Received: June 21, 2023
Revised: August 26, 2023
Accepted: October 11, 2023
Published: October 13, 2023

REFERENCES

1. Becker, P.B., and Hörz, W. (2002). Atp-dependent nucleosome remodeling. Annu. Rev. Biochem. *71*, 247–273. https://doi.org/10.1146/annurev.biochem.71.110601.135400.
2. Hargreaves, D.C., and Crabtree, G.R. (2011). Atp-dependent chromatin remodeling: genetics, genomics and mechanisms. Cell Res. *21*, 396–420. https://doi.org/10.1038/cr.2011.32.
3. Kasten, M.M., Clapier, C.R., and Cairns, B.R. (2011). Snapshot: chromatin remodeling: swi/snf. Cell *144*, 310.e1. https://doi.org/10.1016/j.cell.2011.01.007.
4. Vignali, M., Hassan, A.H., Neely, K.E., and Workman, J.L. (2000). Atp-dependent chromatin-remodeling complexes. Mol. Cell Biol. *20*, 1899–1910. https://doi.org/10.1128/MCB.20.6.1899-1910.2000.
5. Kwon, C.S., and Wagner, D. (2007). Unwinding chromatin for development and growth: a few genes at a time. Trends Genet. *23*, 403–412. https://doi.org/10.1016/j.tig.2007.05.010.
6. Roberts, C.W.M., and Orkin, S.H. (2004). The swi/snf complex–chromatin and cancer. Nat. Rev. Cancer *4*, 133–142. https://doi.org/10.1038/nrc1273.
7. Ryme, J., Asp, P., Böhm, S., Cavellán, E., and Farrants, A.Ö. (2009). Variations in the composition of mammalian swi/snf chromatin remodelling complexes. J. Cell. Biochem. *108*, 565–576. https://doi.org/10.1002/jcb.22288.
8. Debril, M.B., Gelman, L., Fayard, E., Annicotte, J.S., Rocchi, S., and Auwerx, J. (2004). Transcription factors and nuclear receptors interact with the swi/snf complex through the baf60c subunit. J. Biol. Chem. *279*, 16677–16686. https://doi.org/10.1074/jbc.M312288200.
9. Hsiao, P.W., Fryer, C.J., Trotter, K.W., Wang, W., and Archer, T.K. (2003). Baf60a mediates

critical interactions between nuclear receptors and the brg1 chromatin-remodeling complex for transactivation. Mol. Cell Biol. *23*, 6210–6220. https://doi.org/10.1128/MCB.23.17.6210-6220.2003.

10. Ito, T., Yamauchi, M., Nishina, M., Yamamichi, N., Mizutani, T., Ui, M., Murakami, M., and Iba, H. (2001). Identification of swi·snf complex subunit baf60a as a determinant of the transactivation potential of fos/jun dimers. J. Biol. Chem. *276*, 2852–2857. https://doi.org/10.1074/jbc.M009633200.
11. Li, S., Liu, C., Li, N., Hao, T., Han, T., Hill, D.E., Vidal, M., and Lin, J.D. (2008). Genome-wide coactivation analysis of pgc-1alpha identifies baf60a as a regulator of hepatic lipid metabolism. Cell Metab. *8*, 105–117. https://doi.org/10.1016/j.cmet.2008.06.013.
12. Lickert, H., Takeuchi, J.K., von Both, I., Walls, J.R., Mcauliffe, F., Adamson, S.L., Henkelman, R.M., Wrana, J.L., Rossant, J., and Bruneau, B.G. (2004). Baf60c is essential for function of baf chromatin remodelling complexes in heart development. Nature *432*, 107–112. https://doi.org/10.1038/nature03071.
13. Wang, W., Xue, Y., Zhou, S., Kuo, A., Cairns, B.R., and Crabtree, G.R. (1996). Diversity and specialization of mammalian swi/snf complexes. Genes Dev. *10*, 2117–2130. https://doi.org/10.1101/gad.10.17.2117.
14. Tao, W., Chen, S., Shi, G., Guo, J., Xu, Y., and Liu, C. (2011). Switch/sucrose nonfermentable (swi/snf) complex subunit baf60a integrates hepatic circadian clock and energy metabolism. Hepatology *54*, 1410–1420. https://doi.org/10.1002/hep.24514.
15. Oh, J., Sohn, D.H., Ko, M., Chung, H., Jeon, S.H., and Seong, R.H. (2008). Baf60a interacts with p53 to recruit the swi/snf complex. J. Biol. Chem. *283*, 11924–11934. https://doi.org/10.1074/jbc.M705401200.
16. Nakamura, R., Koshiba-Takeuchi, K., Tsuchiya, M., Kojima, M., Miyazawa, A., Ito, K., Ogawa, H., and Takeuchi, J.K. (2016). Expression analysis of baf60c during heart regeneration in axolotls and neonatal mice. Dev. Growth Differ. *58*, 367–382. https://doi.org/10.1111/dgd.12281.
17. Takeuchi, J.K., and Bruneau, B.G. (2009). Directed transdifferentiation of mouse mesoderm to heart tissue by defined factors. Nature *459*, 708–711. https://doi.org/10.1038/nature08039.
18. Forcales, S.V., Albini, S., Giordani, L., Malecova, B., Cignolo, L., Chernov, A., Coutinho, P., Saccone, V., Consalvi, S., Williams, R., et al. (2012). Signal-dependent incorporation of myod-baf60c into brg1-based swi/snf chromatin-remodelling complex. EMBO J. *31*, 301–316. https://doi.org/10.1038/emboj.2011.391.
19. Goljanek-Whysall, K., Mok, G.F., Fahad Alrefaei, A., Kennerley, N., Wheeler, G.N., and Münsterberg, A. (2014). Myomir-dependent switching of baf60 variant incorporation into brg1 chromatin remodeling complexes during embryo myogenesis. Development *141*, 3378–3387. https://doi.org/10.1242/dev.108787.
20. Saccone, V., Consalvi, S., Giordani, L., Mozzetta, C., Barozzi, I., Sandoná, M., Ryan, T., Rojas-Muñoz, A., Madaro, L., Fasanaro, P., et al. (2014). Hdac-regulated myomirs control baf60 variant exchange and direct the functional phenotype of fibro-adipogenic progenitors in dystrophic muscles. Genes Dev. *28*, 841–857. https://doi.org/10.1101/gad.234468.113.
21. Meng, Z.X., Li, S., Wang, L., Ko, H.J., Lee, Y., Jung, D.Y., Okutsu, M., Yan, Z., Kim, J.K., and Lin, J.D. (2013). Baf60c drives glycolytic metabolism in the muscle and improves systemic glucose homeostasis through deptor-mediated akt activation. Nat. Med. *19*, 640–645. https://doi.org/10.1038/nm.3144.
22. Meng, Z.X., Wang, L., Xiao, Y., and Lin, J.D. (2014). The baf60c/deptor pathway links skeletal muscle inflammation to glucose homeostasis in obesity. Diabetes *63*, 1533–1545. https://doi.org/10.2337/db13-1061.
23. Zhu, G., and Lee, A.S. (2015). Role of the unfolded protein response, grp78 and grp94 in organ homeostasis. J. Cell. Physiol. *230*, 1413–1420. https://doi.org/10.1002/jcp.24923.
24. Goldenberg-Cohen, N., Raiter, A., Gaydar, V., Dratviman-Storobinsky, O., Goldstein, T., Weizman, A., and Hardy, B. (2012). Peptide-binding grp78 protects neurons from hypoxia-induced apoptosis. Apoptosis *17*, 278–288. https://doi.org/10.1007/s10495-011-0678-x.
25. Jiang, C.C., Chen, L.H., Gillespie, S., Wang, Y.F., Kiejda, K.A., Zhang, X.D., and Hersey, P. (2007). Inhibition of mek sensitizes human melanoma cells to endoplasmic reticulum stress-induced apoptosis. Cancer Res. *67*, 9750–9761. https://doi.org/10.1158/0008-5472.CAN-07-2047.
26. Kim, R., Emi, M., Tanabe, K., and Murakami, S. (2006). Role of the unfolded protein response in cell death. Apoptosis *11*, 5–13. https://doi.org/10.1007/s10495-005-3088-0.
27. Shu, C.W., Sun, F.C., Cho, J.H., Lin, C.C., Liu, P.F., Chen, P.Y., Chang, M.D.T., Fu, H.W., and Lai, Y.K. (2008). Grp78 and raf-1 cooperatively confer resistance to endoplasmic reticulum stress-induced apoptosis. J. Cell. Physiol. *215*, 627–635. https://doi.org/10.1002/jcp.21340.
28. Li, J., Ni, M., Lee, B., Barron, E., Hinton, D.R., and Lee, A.S. (2008). The unfolded protein response regulator grp78/bip is required for endoplasmic reticulum integrity and stress-induced autophagy in mammalian cells. Cell Death Differ. *15*, 1460–1471. https://doi.org/10.1038/cdd.2008.81.
29. Shintani, T., and Klionsky, D.J. (2004). Autophagy in health and disease: a double-edged sword. Science *306*, 990–995. https://doi.org/10.1126/science.1099993.
30. Wang, Y., Wu, H., Li, Z., Yang, P., and Li, Z. (2017). A positive feedback loop between grp78 and vps34 is critical for grp78-mediated autophagy in cancer cells. Exp. Cell Res. *351*, 24–35. https://doi.org/10.1016/j.yexcr.2016.12.017.
31. Dauer, P., Sharma, N.S., Gupta, V.K., Durden, B., Hadad, R., Banerjee, S., Dudeja, V., Saluja, A., and Banerjee, S. (2019). Er stress sensor, glucose regulatory protein 78 (grp78) regulates redox status in pancreatic cancer thereby maintaining "stemness". Cell Death Dis. *10*, 132. https://doi.org/10.1038/s41419-019-1408-5.
32. Lee, A.S. (2014). Glucose-regulated proteins in cancer: molecular mechanisms and therapeutic potential. Nat. Rev. Cancer *14*, 263–276. https://doi.org/10.1038/nrc3701.
33. Li, Z., and Li, Z. (2012). Glucose regulated protein 78: a critical link between tumor microenvironment and cancer hallmarks. Biochim. Biophys. Acta *1826*, 13–22. https://doi.org/10.1016/j.bbcan.2012.02.001.
34. Contreras, C., González-García, I., Martínez-Sánchez, N., Seoane-Collazo, P., Jacas, J., Morgan, D.A., Serra, D., Gallego, R., Gonzalez, F., Casals, N., et al. (2014). Central ceramide-induced hypothalamic lipotoxicity and ER stress regulate energy balance. Cell Rep. *9*, 366–377. https://doi.org/10.1016/j.celrep.2014.08.057.
35. Kammoun, H.L., Chabanon, H., Hainault, I., Luquet, S., Magnan, C., Koike, T., Ferré, P., and Foufelle, F. (2009). Grp78 expression inhibits insulin and ER stress-induced srebp-1c activation and reduces hepatic steatosis in mice. J. Clin. Invest. *119*, 1201–1215. https://doi.org/10.1172/JCI37007V.
36. Lin, J., Jiang, X., Dong, M., Liu, X., Shen, Q., Huang, Y., Zhang, H., Ye, R., Zhou, H., Yan, C., et al. (2021). Hepatokine pregnancy zone protein governs the diet-induced thermogenesis through activating brown adipose tissue. Adv. Sci. *8*, e2101991. https://doi.org/10.1002/advs.202101991.
37. Thon, M., Hosoi, T., and Ozawa, K. (2016). Insulin enhanced leptin-induced stat3 signaling by inducing grp78. Sci. Rep. *6*, 34312. https://doi.org/10.1038/srep34312.
38. Misra, U.K., Kaczowka, S., and Pizzo, S.V. (2010). Inhibition of NF-κB1 and NF-κB2 activation in prostate cancer cells treated with antibody against the carboxyl terminal domain of grp78: effect of p53 upregulation. Biochem. Biophys. Res. Commun. *392*, 538–542. https://doi.org/10.1016/j.bbrc.2010.01.058.
39. Qin, K., Ma, S., Li, H., Wu, M., Sun, Y., Fu, M., Guo, Z., Zhu, H., Gong, F., Lei, P., and Shen, G. (2017). Grp78 impairs production of lipopolysaccharide-induced cytokines by interaction with cd14. Front. Immunol. *8*, 579. https://doi.org/10.3389/fimmu.2017.00579.
40. Zhou, X., Yang, M., Lv, Y., Li, H., Wu, S., Min, J., Shen, G., He, Y., and Lei, P. (2021). Adoptive transfer of grp78-treated dendritic cells alleviates insulitis in nod mice. J. Leukoc. Biol. *110*, 1023–1031. https://doi.org/10.1002/JLB.3MA0921-219RRRR.
41. Hotamisligil, G.S. (2006). Inflammation and metabolic disorders. Nature *444*, 860–867. https://doi.org/10.1038/nature05485.
42. Li, X., Jiang, Y., Liu, W., and Ge, X. (2012). Protein-sparing effect of dietary lipid in practical diets for blunt snout bream (*Megalobrama amblycephala*) fingerlings: effects on digestive and metabolic responses. Fish Physiol. Biochem. *38*, 529–541. https://doi.org/10.1007/s10695-011-9533-9.
43. Yan, J., Liao, K., Wang, T., Mai, K., Xu, W., and Ai, Q. (2015). Dietary lipid levels influence lipid deposition in the liver of large yellow croaker (*Larimichthys crocea*) by regulating lipoprotein receptors, fatty acid uptake and triacylglycerol synthesis and catabolism at the transcriptional level. PLoS One *10*, e0129937. https://doi.org/10.1371/journal.pone.0129937.
44. Wang, T., Yan, J., Xu, W., Ai, Q., and Mai, K. (2016). Characterization of Cyclooxygenase-2 and its induction pathways in response to high lipid diet-induced inflammation in *Larmichthys crocea*. Sci. Rep. *6*, 19921. https://doi.org/10.1038/srep19921.
45. Cai, W., Albini, S., Wei, K., Willems, E., Guzzo, R.M., Tsuda, M., Giordani, L., Spiering, S., Kurian, L., Yeo, G.W., et al. (2013). Coordinate nodal and bmp inhibition directs baf60c-dependent cardiomyocyte commitment. Genes Dev. *27*, 2332–2344. https://doi.org/10.1101/gad.225144.113V.
46. Forcales, S.V. (2012). The baf60c-myod complex poises chromatin for rapid

transcription. BioArchitecture *2*, 104–109. https://doi.org/10.4161/bioa.20970.

47. Wang, Y., Wong, R.H.F., Tang, T., Hudak, C.S., Yang, D., Duncan, R.E., and Sul, H.S. (2013). Phosphorylation and recruitment of baf60c in chromatin remodeling for lipogenesis in response to insulin. Mol. Cell *49*, 283–297. https://doi.org/10.1016/j.molcel.2012.10.028.
48. Wang, X., Wu, X., Wang, Q., Zhang, Y., Wang, C., and Chen, J. (2020). NLRP6 suppresses gastric cancer growth via GRP78 ubiquitination. Exp. Cell Res. *395*, 112177. https://doi.org/10.1016/j.yexcr.2020.112177.
49. Yang, L., Dai, R., Wu, H., Cai, Z., Xie, N., Zhang, X., Shen, Y., Gong, Z., Jia, Y., Yu, F., et al. (2022). Unspliced XBP1 Counteracts β-Catenin to Inhibit Vascular Calcification. Circ. Res. *130*, 213–229. https://doi.org/10.1161/CIRCRESAHA.121.319745.
50. Ferguson, L.P., Gatchalian, J., Mcdermott, M.L., Nakamura, M., Chambers, K., Rajbhandari, N., Lytle, N.K., Rosenthal, S.B., Hamilton, M., Albini, S., et al. (2023). Smarcd3 is an epigenetic modulator of the metabolic landscape in pancreatic ductal adenocarcinoma. Nat. Commun. *14*, 292. https://doi.org/10.1038/s41467-023-35796-7.
51. Meng, Z.X., Wang, L., Chang, L., Sun, J., Bao, J., Li, Y., Chen, Y.E., and Lin, J.D. (2015). A diet-sensitive baf60a-mediated pathway links hepatic bile acid metabolism to cholesterol absorption and atherosclerosis. Cell Rep. *13*, 1658–1669. https://doi.org/10.1016/j.celrep.2015.10.033.
52. Contreras, C., González-García, I., Seoane-Collazo, P., Martínez-Sánchez, N., Liñares-Pose, L., Rial-Pensado, E., Fernø, J., Tena-Sempere, M., Casals, N., Diéguez, C., et al. (2017). Reduction of hypothalamic endoplasmic reticulum stress activates browning of white fat and ameliorates obesity. Diabetes *66*, 87–99. https://doi.org/10.2337/db15-1547.
53. Suzuki, T., Lu, J., Zahed, M., Kita, K., and Suzuki, N. (2007). Reduction of grp78 expression with siRNA activates unfolded protein response leading to apoptosis in hela cells. Arch. Biochem. Biophys. *468*, 1–14. https://doi.org/10.1016/j.abb.2007.09.004.
54. Fang, W., Chen, Q., Cui, K., Chen, Q., Li, X., Xu, N., Mai, K., and Ai, Q. (2021). Lipid overload impairs hepatic vldl secretion via oxidative stress-mediated pkcdelta-hnf4alpha-mtp pathway in large yellow croaker (*larimichthys crocea*). Free Radic. Biol. Med. *172*, 213–225. https://doi.org/10.1016/j.freeradbiomed.2021.06.001.
55. Cui, K., Li, Q., Xu, D., Zhang, J., Gao, S., Xu, W., Mai, K., and Ai, Q. (2020). Establishment and characterization of two head kidney macrophage cell lines from large yellow croaker (*larimichthys crocea*). Dev. Comp. Immunol. *102*, 103477. https://doi.org/10.1016/j.dci.2019.103477.
56. Livak, K.J., and Schmittgen, T.D. (2001). Analysis of relative gene expression data using real-time quantitative PCR and the 2-ddct method. Methods *25*, 402–408. https://doi.org/10.1006/meth.2001.1262.
57. Yang, B., Zhou, Y., Wu, M., Li, X., Mai, K., and Ai, Q. (2020). Ω-6 polyunsaturated fatty acids (linoleic acid) activate both autophagy and antioxidation in a synergistic feedback loop via tor-dependent and tor-independent signaling pathways. Cell Death Dis. *11*, 607. https://doi.org/10.1038/s41419-020-02750-0.
58. Chen, Q., Du, J., Cui, K., Fang, W., Zhao, Z., Chen, Q., Mai, K., and Ai, Q. (2021). Acetyl-CoA derived from hepatic mitochondrial fatty acid beta-oxidation aggravates inflammation by enhancing p65 acetylation. iScience *24*, 103244. https://doi.org/10.1016/j.isci.2021.103244.
59. Du, J., Chen, Q., Li, Y., Xiang, X., Xu, W., Mai, K., and Ai, Q. (2020). Activation of the farnesoid x receptor (FXR) suppresses linoleic acid-induced inflammation in the large yellow croaker (*larimichthys crocea*). J. Nutr. *150*, 2469–2477. https://doi.org/10.1093/jn/nxaa185.

STAR★METHODS

KEY RESOURCES TABLE

REAGENT or RESOURCE	SOURCE	IDENTIFIER
Antibodies		
Rabbit polyclonal Anti-BAF60c	This paper	N/A
Rabbit monoclonal Anti-GRP78	Cell Signaling Technology	CAT#3177; RRID: AB_2119845
Rabbit polyclonal Anti-JNK1/2	Cell Signaling Technology	CAT#9252; RIDD: AB_2250373
Rabbit monoclonal Anti-p-JNK1/2	Cell Signaling Technology	CAT#4668; RIDD: AB_823588
Rabbit polyclonal Anti-eIF2α	Cell Signaling Technology	CAT#9722
Rabbit polyclonal Anti-p-eIF2α	Cell Signaling Technology	CAT#9721
Rabbit monoclonal Anti-ERK1/2	Cell Signaling Technology	CAT#4695; RIDD: AB_390779
Rabbit monoclonal Anti-p-ERK1/2	Cell Signaling Technology	CAT#4370; RIDD: AB_2315112
Rabbit monoclonal Anti-DYKDDDDK Tag	Cell Signaling Technology	CAT#14793; RRID: AB_2572291
Rabbit monoclonal Anti-HA Tag	Cell Signaling Technology	CAT#3724; RRID: AB_1549585
Mouse polyclonal Anti-GAPDH	Golden Bridge Biotechnology	CAT#TA-08
Bacterial and virus strains		
Escherichia coli-DH5α	TransGen Biotech	CAT#CD201-01
Chemicals, peptides, and recombinant proteins		
Bip Inducer X	MedChemExpress	CAT#HY-110188
HM03	MedChemExpress	CAT#HY-125974
EZ Trans transfection reagent	LIFE iLAB	CAT#AC04L099
Critical commercial assays		
TranscriptAid T7 High Yield Transcription Kit	Thermo Fisher Scientific	CAT#K0441
Deposited data		
The RNA sequence data	This paper	BioProject: PRJNA1004361
Experimental models: Cell lines		
Human: HEK293T cell line	ATCC	CAT#CRL-3216
Large yellow croaker: primary hepatocytes	This paper	N/A
Large yellow croaker: macrophage cell line	(Cui et al., 2020)[55]	N/A
Experimental models: Organisms/strains		
Juvenile large yellow croaker	NingdeFufa Fishery Co., Ltd. (China)	N/A
Oligonucleotides		
Primers for qRT-PCR, see Table S1	This paper	N/A
Primers for recombinant DNA, see Table S1	This paper	N/A
Recombinant DNA		
pCDNA3.1(+)	Miaoling Bio	CAT#P0157
PCS2+	KeLeiBio	kl-zl-0892
Plasmid: pCDNA3.1(+)-BAF60c-GFP	This paper	N/A
Plasmid: pCDNA3.1(+)-GRP78-RFP	This paper	N/A
Plasmid: PCS2+-BAF60c-HA	This paper	N/A
Plasmid: PCS2+-GRP78-FLAG	This paper	N/A
Plasmid: Lamin A/C-RFP	This paper	N/A
Software and algorithms		
GraphPad Prim 7.0	GraphPad Software	https://www.graphpad.com/
Image J	NIH	https://imagej.nih.gov/ij/

RESOURCE AVAILABILITY

Lead contact

Further information and requests for resources and reagents should be directed to and will be fulfilled by the lead contact, Qinghui Ai (qhai@ouc.edu.cn).

Materials availability

Materials generated in this study are available from the lead contact upon reasonable request.

Data and code availability

- All relevant data are within the manuscript and Supplementary Material. The accession number for the RNA sequencing data reported in this paper is PRJNA1004361.
- This paper does not report original code.
- Any additional information required to reanalyze the data reported in this paper is available from the lead contact upon request.

EXPERIMENTAL MODEL AND STUDY PARTICIPANT DETAILS

Animals and diets

Husbandry and handling of fish in this study were performed strictly according to the Management Rule of Laboratory Animals (Chinese Order No. 676 of the State Council, revised 1 March 2017).

Large yellow croaker juveniles were obtained from NingdeFufa Fishery Co., Ltd. (China). The control group was fed a diet containing a moderate level of crude lipids (12%), and the high fat diet (HFD) group was fed a lipid-rich diet (18%). The formulation and proximate composition of diets used in the present study were according to the previous study.[54] In the study, both sexes were used. After 10 weeks of feeding experiment, fish were fasted for 24 h and then used for the injection experiments.

The dsRNA (Double stranded RNA) used for BAF60c knockdown was synthesized using TranscriptAid T7 High Yield Transcription Kit (Thermofisher, USA) following the manufacturer's protocol. Fish in the control group and HFD group were administered intraperitoneally injections of dsRNA-BAF60c at a dose of 2 μg/ (g b.w) or equivalent volumes of dsRNA-control for 36 h, respectively. The liver and head kidney were collected and stored at -80°C for subsequent analysis. Moreover, the liver was stored in Glutaraldehyde, 2.5% (EM Grade) (Solarbio, China) for Transmission electron microscopy analysis.

Cell culture and treatment

Livers of juvenile yellow croakers were removed and placed in sterile phosphate buffer (PBS, Vivacell, China) containing penicillin and streptomycin (cat. no. P1400, Solarbio, China). After washing with Dulbecco's modified Eagle medium/Ham's F12 medium (1:1) (DMEM/F12, Vivacell, China), the liver tissue was chopped into 1-mm^3 slices and digested with 0.25% trypsin (Thermo Fisher Scientific, USA) for 10 min. After neutralization with DMEM/F12 medium containing fetal bovine serum (FBS, Procell, China), the cell precipitate was suspended in complete medium composed of DMEM/F12 medium supplemented with 15% FBS, 100 U penicillin and 100 mg/mL streptomycin. The cell suspension was inoculated into a six-well culture plate and incubated at 28°C. The macrophage line of large yellow croaker was provided by our colleagues.[55] Briefly, cells were inoculated into 12-well or 6-well plates at a density of 1.0×10^6 cells/ml and were cultured in DMEM/F12 medium (VivaCell, China) with 15% FBS (Procell, China) and 1% antibiotics (Solarbio, China) at 28°C and 5% CO_2. HEK293T cells were cultured in high-glucose DMEM with 10% FBS and 1% antibiotics at 37°C and 5 % CO_2. GRP78 agonist (Bip inducer X; MCE) and GRP78 inhibitor (HM03; MCE) were incubated with a concentration of 10 μM for different time points. BAF60c-siRNA and BAF60c-GFP plasmid were electroporated into macrophages/hepatocytes to knockdown and overexpression of BAF60c, respectively. After treatment, cells were lysed in the wells and harvested for subsequent analysis.

METHOD DETAILS

RNA isolation and quantitative real-time PCR

Total RNA was extracted by Trizol reagent (Takara, China) according to the manufacturer's protocol. The quality of RNA was measured through electrophoresis using 1.2% denatured agarose gel. cDNA synthesis was performed by PrimeScript RT reagent kit (Takara, China) following the manufacturer's instructions. The mRNA levels were measured using a quantitative thermal cycler (Bio-rad, USA) by SYBR Green real-time PCR kit (Takara, China), the primers used were listed in Table S1. The levels of each gene were normalized to that of *β-actin* using the $2^{-\Delta\Delta ct}$ method.[56]

Gene cloning and sequence analysis

Primers used for amplification of complete CDS were designed according to the predicted sequence of large yellow croaker *baf60c* (GenBank: XM_019271685.2). The DNAMAN software was used to analyze multiple alignments of amino acid sequences from different species. The phylogenetic tree was constructed by the neighbor-joining method using MEGAX.

Plasmid construction

Baf60c of large yellow croaker was cloned into the pcDNA3.1-GFP or pCS2+ vector using a ClonExpress II One Step Cloning Kit (Vazyme, China). Then, *grp78* was cloned into pcDNA3.1-RFP or pCS2+ vector. Specific primers were designed to insert HA tag and FLAG tag into pCS2+-BAF60c and pCS2+-GRP78 plasmids, respectively. The Lamin A/C-RFP plasmid was stored in our laboratory.

Subcellular localization, colocalization, and transmission electron microscopy (TEM) observation

For subcellular localization analysis use, HEK293T cells were co-transfected with BAF60c-GFP and Lamin A/C-RFP plasmids using EZ Trans (Life iLab, China) for 24 h in confocal dishes. HEK293T cells were co-transfected with the BAF60c-GFP and GRP78-RFP plasmids for 24 h in confocal dishes for colocalization analysis. Then cells were visualized by laser scanning confocal microscope (Leica, Germany). TEM observation was conducted following the previously described protocol.[57] Briefly, tissue specimens were fixed with 2.5% glutaraldehyde in 0.1 M sodium phosphate buffer (pH 7.2) for 3 h at 4°C, washed in the same buffer for 1 h at 4°C and postfixed with 1% osmium tetroxide in sodium phosphate buffer for 1 h at 4°C. The tissues were then dehydrated in a graded series of ethanol starting at 50% (for 10 min per step) after two washes in propylene oxide. The tissue specimens were embedded in araldite. Ultrathin sections were stained with Mg-uranyl acetate and lead citrate for TEM evaluation.

HIS-pulldown, LC-MS/MS analysis, and RNA sequencing (RNA-Seq)

To identify additional BAF60c-interacting factors, we performed HIS pulldown using purified HIS-tag fusion BAF60c protein followed by LC-MS/MS analysis (Gene Create, China). Bacterially expressed HIS-tag fusion BAF60c protein on Ni-beads were incubated with large yellow croaker liver extracted proteins. Then, the proteins were separated by SDS-PAGE for further LC-MS/MS analysis.

Total RNA was extracted using TRIzol Reagent (Invitrogen, USA) according to the manufacturer's instructions. The RNA quantity was determined by Agilent 2100 Bioanaylzer (Agilent Technologies, USA) and quantified using the NanoDrop 2000 (Thermo Fisher Scientific, USA). After that, RNA sample of high-quality was used for sequencing library construction. By using Illumina HiSeq X10 (Illumina, San Diego, CA), the following RNA reverse transcription, library construction and the sequencing were accomplished at Majorbio Bio-pharm Biotechnology Co., Ltd (Shanghai, China). The data were analyzed on the Majorbio Cloud Platform (Majorbio Bio-pharm Biotechnology, China).

Coimmunoprecipitation (co-IP)

The co-IP experiment was carried out following the protocol as previously described.[58,59] Briefly, HEK293T cells transfected with BAF60c-HA and GRP78-FLAG plasmids were harvested at 24 h. Then, cells were lysed with Cell lysis buffer for Western and IP (Beyotime, China) at 4°C for 20 min, and the lysate was collected by centrifugation to get the supernatant. The supernatant was incubated with Pierce ANTI-HA agarose (Thermo Fisher Scientific, USA), ANTI-FLAG M2 Affinity Gel (Sigma, USA), and IgG-beads (Sigma, USA) at 4°C for 4 h. After washing, we used a HA peptide (MedChem Express, USA) or Flag peptide (MedChem Express) to detach the proteins from agarose beads for further analysis.

Western blotting

Total proteins were extracted from hepatocytes and macrophages using RIPA lysis buffer with protease inhibitors and phosphatase inhibitors. Protein concentrations were determined with a BCA Protein Assay Kit (Beyotime Biotechnology, China) according to the manufacturer's instructions. After standardization, the samples were separated by SDS-PAGE and transferred to 0.45 μm PVDF membranes (Millipore, USA). Membranes were blocked with 5% nonfat dry milk in TBST for 2 h and were then incubated with primary antibodies overnight. Subsequently, the membranes were incubated with secondary antibodies for 1 h and developed with Beyo ECL Plus Reagent (Beyotime Biotechnology, China). The details of antibodies in the present study were listed in the key resources table. The densities of target bands were quantified using the Image J Pro 1.52 software (National Institutes of Health, Bethesda, Maryland, USA) and then normalized to that of GAPDH.

TG contents determination

TG contents were measured using commercial assay kits (Applygen Technologies Inc, Beijing, China), according to manufacturer's instructions.

QUANTIFICATION AND STATISTICAL ANALYSIS

The results were presented as means ± SEM. All data were evaluated by independent *t*-test with the help of SPSS 19.0. $P < 0.05$ was considered to have a significant difference, $P < 0.01$ was highly significant difference. The number of replicates for each experiment are indicated in the figure legends.